Surface-enhanced Raman scattering based on pyramid shaped plasmonic nano-particles in graphene layer

SEYED ENAYATOLLAH TAGHAVI MOGHADDAM*, FARZIN EMAMI*
Opto-Electronic Department of Shiraz University of Technology, Shiraz, Iran

In this paper, the plasmonic effect of gold nanoparticles on graphene-based plasmonic waveguide to improve the nonlinear effect of Raman scattering is investigated. SERS has been explored extensively for applications in sensing and imaging, but the design and optimization of efficient substrates are still challenging. In order to understand and optimize the SERS process in nanoparticles, a novel pyramid shaped gold nanoparticle was synthesized in a graphene layer and characterized according to their average size, zeta potential and UV/visible absorption. In fact, in this research, an asymmetric new plasmonic nano-particle is proposed and designed as pyramid shaped gold nanoparticles in graphene layer. With the help of this new nanoparticle, we design and recommend a Raman booster so that the effect of Raman is improved noticeably. It will be shown that using the proposed nano-particle of gold-pyramid-shaped, the absorbance, and intensity of raman booster is improved noticeably.

(Received October 27, 2021; accepted April 5, 2023)

Keywords: Raman scattering, Plasmonics, Graphene, Absorption

1. Introduction

Normally, absorption in optics is known to be a malignant effect that should be reduced. However, absorption, and especially the control of absorption in waveguides, can also be recognized as a useful effect. For example, in a coupling ring resonator inside the ring, it is one hundred percent possible to control the absorption inside the ring [1]. Another example is the importance of absorption in electro-optic modulators [2]. Moreover, absorption control is of particular importance in bio-optics, as recent research on cancer treatment has used absorption control with plasma nanoparticles [3]. The most important advantage of plasmonic nanoparticles over surface plasmons is that they exhibit stronger absorption, scattering, and coupling that occur at visible wavelengths, and their values depend on the geometry of the nanoparticles and the position of the nanoparticles. At the frequency of plasmonic resonance, the absorption of the incoming wave by the nanoparticles is maximized.

In this context, surface-enhanced Raman scattering (SERS) has attractedmuch attention as a sensitive technique for chemical andbioanalytical sensing and imaging [2, 3]. Numerous works have beencarried out todetect SERS effects for different molecules, with different shaped nanoparticles and at different dosages [4], so it is not easy to determine the main parametersthat need to be optimized for effective and reproducible SERS. The development of reliable quantitative comparisons is a priority required for meaningful design strategies for new nanomaterials. Theaim of this study is to identify critical conditions and physical properties of the materials that play the main role in the optimization of SERS. In this work, a novel plasmonic nanoparticle based on gold-DNA-silver is proposed for the first time and it is shown that the Raman scattering absorption coefficient is much higher than that of gold and silver nanoparticles.

Although the SERS effect in metal nanoparticles isthought to originate from the local fields associated with the excitation of the surface plasmon resonances by the Raman source, the nanospheres suffer from low enhancement levels that varygreatly from particle to particle and fluctuate with their environment [5]. Recent explanationsfor SERS on metal nanoparticles are based not only on intrinsic surface plasmons of the nanoparticles, but also on local field "hotspots" due to surface roughness [6,7], between aggregated metallic NPs [8], or between nanoparticles [9] and a metal surface [10] and that the SERS contribution of such hotspots can dominate the observed response [11]. An alternative way to increase the local electromagnetic field associated with SPR is to systematically increase the local shape and material of the nanoparticle. A field strength 10-100 times higher than that at the surface of nanospheres has been estimated at the tips of silver nanotriangles [12]. Recently, a new class of star-shaped gold nanoparticles with sharp edges and tips, called nanostars, was shown to exhibit very high sensitivity to local changes in the dielectric environment as well as greater electric field enhancement around the nanoparticles [13]. Similar results were found for other nanoparticles with sharp features [4, 14].

In [15], label-free detection and fingerprinting of gDNA from Brassicaceae plant species, namely B. juncea and A. thaliana , were investigated using SERS. Additional techniques such as UV-vis absorption, CD spectroscopy, DLS, TEM and zeta potential measurements were used to characterize the synthesized metal NPs and DNA functionalized metal NPs. gDNA was extracted from the young leaf tissue of B. juncea and then added to Ag/Au NPs and their absorption spectrum was monitored. The

structural complexity of SERS metamolecules by increasing the number of nanoparticles and arranging them in complicated configurations is extended in [16]. It is shown that DNA origami metamolecules can precisely localize single dye molecules with Fano resonances (DMFR) and generate quantified surface-enhanced Raman scattering (SERS) [17]. To enable tailored plasmonic permutations, we develop a general and programmable method for anchoring a series of large gold nanoparticles (L-AuNPs) to predetermined n-tuple docking sites of super-origami DNA scaffolds. A tetrameric nanocluster with four spatially organized 80-nm L-AuNPs exhibits peak-and-dip Fano properties.

The methodsfor fabricating gold nanospheres, nanotriangles, and nanostars with a high degree of control over the size/shape distribution can be considered routine,justifying a direct comparison of the SERSefficiencies of the different structures.

Optical properties of thin metal layers and metal nanoparticles are influenced by the coupling of the input electromagnetic field and the coherent motion of the free electron plasma near the metal surface. Plasmon waves can be classified according to their structure (one or two dimensional) and the type of plasmon stimulation [18]:

A. Surface polariton plasmon (SPP) is a two-dimensional propagating wave on a metal-dielectric interface. The electromagnetic field on both sides of the joint season dampens exponentially, limiting the dimensions below the wavelength near the metal surface. In a two-dimensional interface, an SPP is a longitudinal mode with perpendicular wave vector components parallel to the plane. Therefore, the light must have an electric field component on the common chapter plane to excite the SPP.

The SPP wave vector is larger than the light wave vector in the adjacent environment (dielectric). Thus, compared to photonic guided modes, the coupling of light from the open space to the SPP requires a special structural configuration, including a prism or diffraction lattice coupler. SPP, due to its inherent dispersion, is a weak wave that collects the energy of incoming light and amplifies an electric field near the metal surface. On the other hand, ohmic losses of metal shorten the propagation length of SPP and therefore the field limitation and amplification can be changed and corrected by engineering the joint phase structure (in metal or dielectric). By selecting the appropriate structure, it will be possible to fabricate plasmonic waveguides and plasmonic crystals [19] (repeating plasmonic surfaces with a specific pattern).

B - Localized surface plasmons (LSP) - related to the fluctuations of electron plasma in geometric structures limited in dimensions below the wavelength of light (such as metal nanoparticles). LSP resonances depend on the size, shape, and refractive index of the nanoparticle environment. LSPs can be intensively generated with light of appropriate frequency and polarization, regardless of the excitation wave vector. Due to the limited field in the vicinity of nanoparticles, LSP has a low modulus volume and therefore significant field strength, which is limited by ohmic and radiative losses and quantum effects (in ultra-fine particles) [15]. Wavelengths of metal surfaces can also be generated. Therefore, if the resonant frequency of LSP is close to the frequency of SPP resonances, it plays a decisive role in the behavior of SPP on uneven surfaces. Common characteristics of all plasmonic nanostructures are:

- Amplification of the field near the metal surface (compared to the light field entering from the open space);
- Severe sensitivity to refractive index changes in the vicinity of the metal surface;
- Ability to engineer structure and manipulate scattering and resonant frequency by controlling and adjusting the nanostructured body and the surrounding dielectric environment.

The nonlinear effects of light play an important role in various applications of modern optical sciences, including the control of the frequency spectrum of laser light, the production of ultra-short optical pulses, all-optical signal processing, and ultra-fast switching [18]. The nonlinear effects of light are inherently weak because they arise from photon-photon interactions (activated by matter). These interactions are superficially dependent on the intensity of the electromagnetic field and can be amplified in material environments and cause the field amplification process. Extremely high amplitude of the optical response can be achieved with the help of plasmonic effects. These effects are due to the coherent oscillations of free electrons near the noble surface [19]. For large surfaces (in two dimensions) the amplified response is due to SPPs and for metal nanoparticles due to LSPs the resonances depend on the size and shape. Plasmonic stimulation can alter the nonlinear effects of light in a number of ways: 1- Light coupling to surface plasmons can result in strong subjective electromagnetic fields. An important example of this is the surface-reinforced Raman scattering (SERS), in which plasmonic excitations on a rough (or specially engineered) metal surface amplify the weak Raman effect several times [20]. Plasmonic excitations can be extremely sensitive to the dielectric constant of the metal and the surrounding metal. This property is the basis of the operation of plasmon sensors: "Slight changes in refractive index near the metal surface lead to a significant change in plasmon resonance." This high sensitivity can be used to control light with light. Thus, a control beam used a material to induce a nonlinear change in the dielectric properties of one of the materials and controlled the plasmonic resonance and the propagation of the signal beam. Plasmonic stimuli have the ability to respond at very short time scales (several femtoseconds), which allows us to achieve ultra-fast all-optical processing [17].

Basically, the nonlinear effects of light occur when the motion of an electron in a strong electromagnetic field cannot be considered harmonic. Non-harmonic expansion can be written as a series of field strength powers that generate new fields. These components can be propagated in total frequencies and the input field frequency difference in different directions. In practical applications, the most important effects occur in second- and third-order

sentences. The second-order response typically involves the effects of wave composition, leading to the discussion of frequency conversion. The most common example of such effects is SER, in which the input frequency ω becomes its second-order harmonic, 2ω.

In short, nonlinear plasmonics is a relatively emerging field of research, but its basic concepts have been proposed in various ways in the past. Most of the structures proposed so far may be theoretically simple, but their practical implementation is influenced by the limitations of modern nanotechnology technology. Significant advances in the qualitative improvement of devices with very small dimensions, today allow researchers to study and test the principles of nonlinear effects accurately, and in parallel, more elaborate and practical designs by scientists in various sciences Is. The role of plasmonics in triple optics is: Plasmonic nanoparticles have been developed with the help of photonics by amplifying nonlinear effects and applying them at lower optical powers. Plasmonic structures make it possible to reduce the dimensions of optical devices, which play an important role in the integration of photonic components. The response time to plasmonic stimuli is very short, which makes it possible to process and manipulate optical signals at femtosecond time scales. Much of the research in the field of nonlinear plasmonics is devoted to the study of SER, as the laboratory realization of this process is straightforward.

In this paper, we study the nonlinear optical effect of Raman scattering in metal-insulator-metal plasmonic waveguides and propose a new structure for plasmonic waveguides which not only have high nonlinear effect but also high propagation length. The proposed structure has a graphene layer and a pyramid shape of gold nanoparticles.

This paper is organised as follows. In section two, we tend to describe the structure of the proposed waveguide. The theory of the proposed nanoparticles and the optimization method are also presented in this section. In section three, the simulation results of SER in the proposed structure are presented. Section four summarizes the paper.

2. The structure of MGIM waveguide

Fig. 1 shows the structure of the plasmonic waveguide made of graphene MIM in view. As can be seen in the figure, this structure consists of two metal layers at the top and bottom of the structure and a crystal layer of lithium niobite (LiNbO3). A graphene lattice layer is also inserted between the top metal and the crystal layer. The graphene lattice layer leads to a stronger absorption of photons and increases the absorption coefficient in the middle layer, thus increasing the second harmonic production. In addition, a series of pyramid shape nanoparticles of gold were added in the middle of the layer. As we will show, these nanoparticles increase the intensity of the optical field, thus enhancing the second harmonic effect.

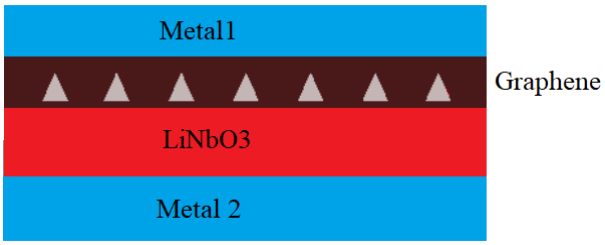

Fig. 1. Structure of the proposed MGIM waveguide under consideration (color online)

The pyramid-shaped gold particles used in this structure with dimensions of 20 to 80 nm and a height of 70 nm with a periodicity of 200 nm were examined. Fig. 2 shows the structure in 3D.

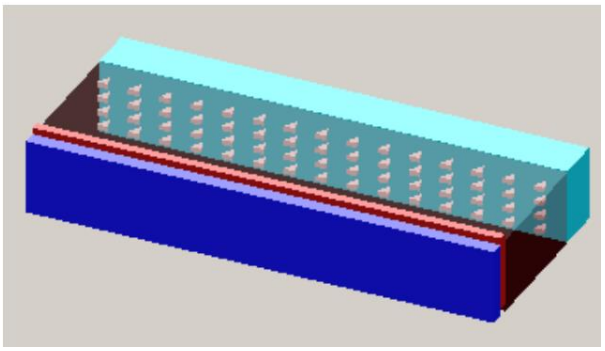

Fig. 2. 3D view of the proposed structure (color online)

There is a comprehensive analytic solution of complex scattering theory for the geometry of finite and specific structures. For example, if we extend the electromagnetic field in terms of spherical harmonics and restrict ourselves to spherical or quasi-spherical nanoparticles, there is an analytical solution to obtain the scattering. However, we would like to exploit the special optical properties and characteristics of non-spherical (arbitrarily shaped) nanoparticles. Thus, we need to look for methods that can model and analyze these particles as well. For this reason, and because of the particular complexity sometimes encountered in computer simulation of analytical methods, we turn to advanced numerical methods. One of the comprehensive methods for the analysis of complex nanostructures is the Discrete-Dipole Approximation (DDA) method [21]. In the DDA method, only the volume of the nanoparticle is discretized and crosslinked, while in the FDTD method, both the particle and its surroundings must be included in the crosslinking process. The May scattering theory is only used in the analysis of spherical particles. The T-matrix method can be applied to any structure of any shape, but firstly its convergence in very large arrays of particles is extremely difficult, and secondly only the scattered field outside the innermost layer of the nanoparticle is calculated. Therefore, the application of this method is limited to the calculation of stray fields in the far-field region and information about the near-field is not available. Due to the above limitations and problems,

the DDA method is valid for far-field and near-field analysis (in two separate experiments) and can be cited [22, 23].

At a glance, it can be seen that DDA solves the problem of electromagnetic scattering of incoming light into a piece in the form of a simple matrix equation (1).

$$\tilde{A}\tilde{P} = \tilde{E}_{\text{inc}} \tag{1}$$

where E_inc show the mixed 3N vector from the input electric field to the N point of the network, P shows the mixed 3N vector from the unknown polarization of the network dipoles, and A shows the mixed matrix with dimensions 3N × 3N. Suppose a point network with N is a point point filled with index j = 1,2,3, .., N to describe the network. Each dipole is defined by the arbitrary index j by the polarization template α_j. If the identical substance is round, α_j is a diameter with the same components (that is, in this particular case, α_j can be thought of as a scalar quantity). We turn our attention to the state in which all α_js can be diagonally diagonally at the same time.

$$P_j = \alpha_j E_{ext,j} \tag{2}$$

This relation can be rewritten in the form of N simultaneous vector equation as follows:

$$P_j = \alpha_j\left(E_{inc,j} - \sum_{j\neq k} A_{jk}P_k\right) \tag{3}$$

where E_ (inc, j) corresponds to the electric field of a flat input wave at location j:

$$E_{inc,j} = E_0 \exp\,(ik.r_j - i\omega t) \tag{4}$$

And $-A_{jk}P_k$ is the share of the electric field in position j according to the polarity of location k. A_jk matrices are also defined as follows:

$$A_{jk} = \frac{e^{ik}r_{jk}}{r_{jk}^3} \times k^2 r_{jk} \times \left(r_{jk} \times P_k\right) + \frac{1-ikr_{jk}}{r_{jk}^2} \times \left[r_{jk}^2 P_k - 3r_{jk}\left(r_{jk} \cdot P_k\right)\right], j \neq k \tag{5}$$

Now, with the introduction of the next two 3N vectors:

$$\tilde{P} = (P_1, P_2, \dots, P_N)$$
$$\tilde{E}_{inc} = \left(\tilde{E}_{inc,1}, \tilde{E}_{inc,2}, \dots, \tilde{E}_{inc,N}\right) \tag{6}$$

There are several ways to solve this system of equations. In this article, a repetitive technique is used. This method starts with an initial guess (typically P˜ = 0) and then in an iterative cycle, improves the initial P estimate step by step until the (1) reaches a certain standard of error. Usually the error variation limits are considered to be less than 10^{-5}.

In certain circumstances, method convergence may be problematic. Therefore, in order to converge the method, the grid size and the step of the iterative steps must be carefully selected. After solving the scattering equation in the matrix form, several parameters are defined to evaluate the optical response of the grid. The most common of these parameters are Extinction cross section, Absorption cross section, and scattering cross section that are defined respectively as follows:

$$C_{ext} = \frac{4\pi k}{|E_{inc}|^2}\sum_{j=1}^{N} Im\{\bar{E}^*_{inc,j}.\ P_j\} \tag{7}$$

$$C_{abs} = \frac{4\pi k}{|E_{inc}|^2}\sum_{j=1}^{N}\left[Im\{P_j.(\alpha_j^{-1})^* P_j^*\} - \frac{2}{3}k^3 P_j.P_j^*\right] \tag{8}$$

$$C_{sca} = C_{ext} - C_{abs} \tag{9}$$

To calculate the cross-sectional coefficients, which are an interpretation of the efficiency of absorption and scattering phenomena in the nanoparticle light response, we can write the relationships for the extinction and scattering cross-section and then obtain the absorption cross-section of the difference between these two parameters. When the adsorption phenomenon is predominant, calculating Csca may be a bit difficult, as Cext and Cabs must be calculated with high accuracy. Also, Csca can be obtained by calculating the radiative power of an oscillating dipole array.

$$C_{sca} = \frac{k^4}{|E_{inc}|^2}\int d\Omega \left|\sum_{j=1}^{N}\left[P_j - \hat{n}(\hat{n}.P_j)\right]e^{-ik\hat{n}.r_j}\right|^2 \tag{10}$$

where n, dΩ and k represent the unit vector in the direction of scattering, the body angle element and the wave number, respectively.

To start modeling and studying the nonlinear effects of SER in the proposed structure and changes of these effects according to the structure and number of plasmonic nanoparticles, as optical input, the structure is stimulated with a monochromatic plane wave (Equation 4). To calculate the bipolar field, the time-harmonic component - iωt is removed from the field equation. The local field due to the excitation input light with polar angle θ and azimuth φ per particle is:

$$E_{inc}(r_s) = E_0 e^{jk.r_s} \tag{11}$$

where

$$k = \frac{2\pi}{\lambda}\hat{k} = \frac{2\pi}{\lambda}[sin(\theta)cos(\phi), sin(\theta)sin(\phi), cos(\theta)] \quad (12)$$

The field with polarization S will be (13) and with polarization P will be (14).

$$E_0 = \left[\cos\left(\varphi + \frac{\pi}{2}\right), \sin\left(\varphi + \frac{\pi}{2}\right), 0\right] \quad (13)$$

$$E_0 = \left[\sin\left(\theta - \frac{\pi}{2}\right) \cdot \cos(\varphi), \sin\left(\theta - \frac{\pi}{2}\right) \cdot \sin(\varphi), \cos\left(\theta - \frac{\pi}{2}\right)\right] \quad (14)$$

When the applied field is parallel to one of the principal axes, the polarizability can be calculated from the following equation:

$$\alpha_s = V\varepsilon_0 \frac{\varepsilon_r - 1}{1 + L_1(\varepsilon_r - 1)} \quad (15)$$

where:

$$\varepsilon_r = \frac{\varepsilon_{particle}}{\varepsilon_{Medium}} \quad (16)$$

ε_r is the relative dielectric function of the particle relative to the environment, and V is the volume of the nanoparticle and L_1 is the shape factor. For particles of arbitrary shape, the following integral relation can be suggested, which is a function of the quasi-axes a, b and c of the nanoparticle.

$$L_1 = \int_0^\infty \frac{a.b.c.ds}{(s+a^2)^{\frac{3}{2}}(s+b^2)^{\frac{1}{2}}(s+c^2)^{\frac{1}{2}}} \quad (17)$$

The instantaneous dipole moment induced in a particle of the equation:

$$P_s = \varepsilon_0 \alpha_s E_{loc}(r_s) \quad (18)$$

where P_s, α_s and E_{loc} (r_s) represent the induced torque, the polarization of the particle located at r_s and the local field, respectively. The local field is derived from two sources, so it is seen as a sum of two components. The combination of these two components results in a local field at both poles:

$$E_{loc,s} = E_{inc,s} + E_{dip,s} = E_0 e^{jkr_s} - \sum_{s \neq h} A_{s,h} P_s \quad (19)$$

3. Simulation results

In this section, simulation results for various nanoparticles including the proposed pyramidal gold nanoparticles, spherical gold nanoparticles, and star-shaped gold nanoparticles are presented. By simulating structures containing single nanoparticles, the absorption spectra of four types of nanoparticles are shown in Figure 3. As can be seen, the absorption of the proposed structure is much higher than other structures.

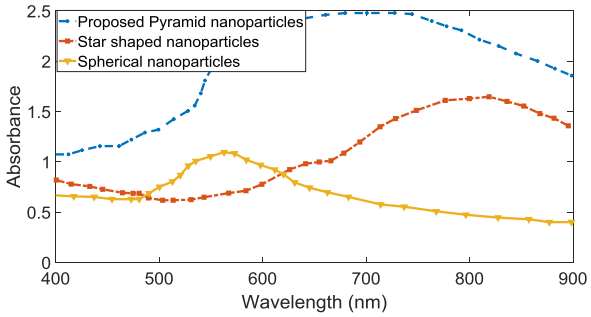

Fig. 3. Different nanoparticle adsorption spectra (color online)

Fig. 4 shows the excited Raman enhancement diagram for different structures. It can be seen that the proposed structure was greatly enhanced by increasing the interest rate. In this figure, the gain diagram is drawn in terms of pump power and the maximum gain is 0.9 dB / cm. Table 1 summarizes the results of these simulations. In this table, the results for silver nanoparticles are included for comparison purposes.

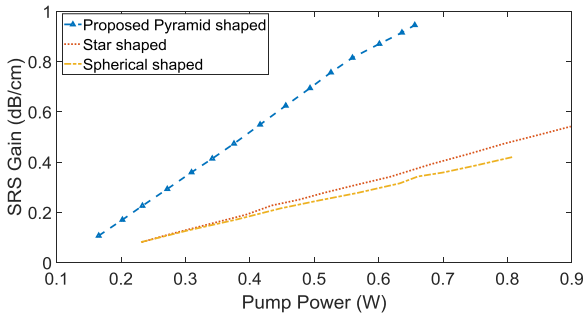

Fig. 4. Stimulated Raman interest diagram for different structures (color online)

Table 1. Results for silver nanoparticles

Intensity	Raman gain	Absorption	Structure
0.46E4	0.28	0.2	silver
0.5E4	0.3	0.6	gold
1.5E4	0.4	1	Star shaped gold
2.5E4	0.5	1.5	Pyramid shaped Silver
3.5E4	0.9	2	Pyramid shaped gold

Also, the number of nanoparticles can change the performance of the structure. Fig. 5 shows the absorption

coefficient diagram for different numbers of pyramid shaped nanoparticles. It can be seen that the number of nanoparticles strongly affects the absorption coefficient and therefore the number of nanoparticles can be optimized to achieve the highest possible absorption coefficient.

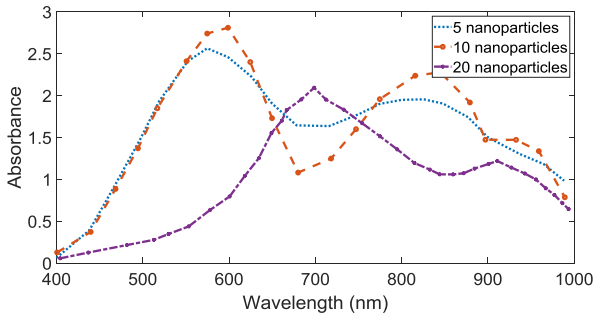

Fig. 5. Absorption coefficient diagram per number of different nanoparticles (color online)

Figs. 6 to 8 show the absorption coefficient and gain and light intensity in terms of the number of nanoparticles. It can be seen that for 35 nanoparticles the values of absorption coefficient, gain and intensity are optimized. It should be noted that the interest rate and absorption coefficient are plotted in this diagram. It should be noted that with 35 nanoparticles, the absorption coefficient and the gain are the maximum, but the intensity is not the maximum, but it has a high and acceptable value. Therefore, we choose 35 as the optimal number.

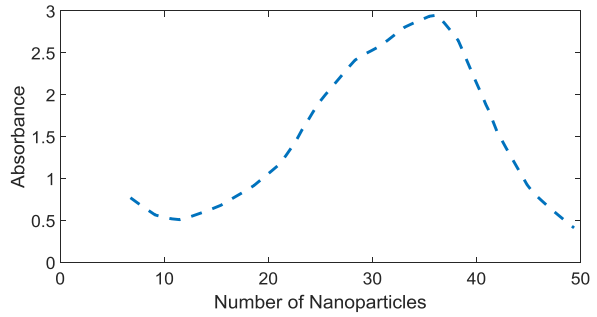

Fig. 6. Graph of absorption coefficient in terms of number of nanoparticles (color online)

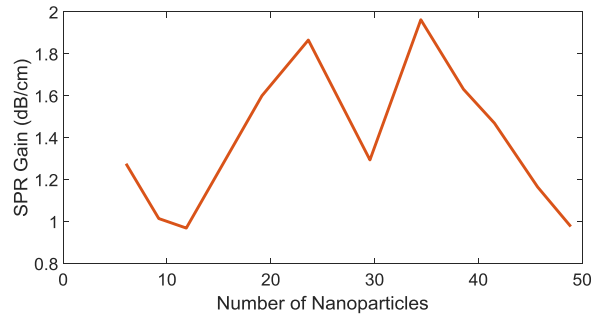

Fig. 7. Raman gain diagram in terms of number of nanoparticles (color online)

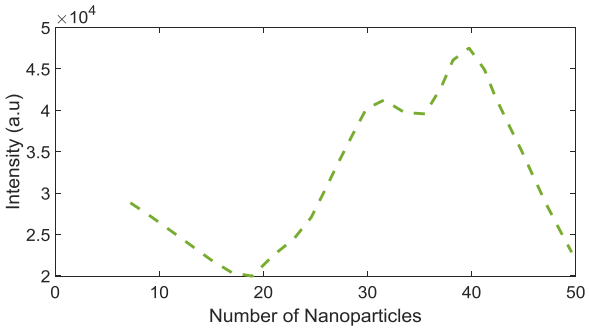

Fig. 8. Intensity diagram in terms of number of nanoparticles (color online)

In addition to nanoparticles, the thickness of the structural layers, including the graphene layer, can also affect the performance of the Raman amplifier. To illustrate this, the thickness of this layer, which has so far been considered 2.5 nm, is changed from 1nm to 5nm. Fig. 9 shows the simulation results of this work. It can be seen that the thickness of the graphene layer has a great effect on the performance of the amplifier and for a thickness of 3 nm, the maximum absorption coefficient is 3.3.

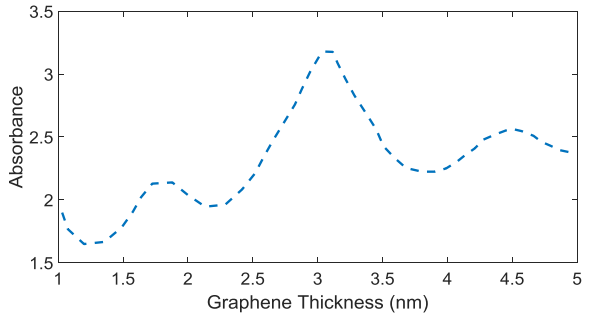

Fig. 9. Absorption coefficient in terms of graphene layer thickness (color online)

4. Conclusions

This study introduced a pyramidal gold plasmonic nanoparticle in a graphene layer and showed that the field strength and absorption coefficient are 100 times higher than the previously reported structures. In fact, the use of pyramidal gold nanoparticles in a layer of graphene causes a very high absorption. The most important advantage of plasmonic nanoparticles over surface plasma is that they have the property of absorbing, scattering and pairing at visible wavelengths. The value of these parameters depends on the geometry and position of the nanoparticles. Equations and modeling have been used in the simulations of the relations and models of Chapter Five. The absorption of nanoparticles from the input wave is maximized at the plasmonic resonance frequency. It was also shown that in addition to the shape and type of nanoparticles, the number of nanoparticles and the

thickness of the graphene layer have a very strong effect on the absorption coefficient, Raman gain and light intensity.

References

[1] H. MazhabJafari, L. Soleymani, R. Genov, IEEE Trans. Biomed. Circuits Syst. **6**(5), 468 (2012).
[2] J. Kim, R. Maitra, K. D. Pedrotti, W. B. Dunbar, IEEE Trans. Biomed. Circuits Syst. **7**(3), 285 (2013).
[3] L. Kari, M. Daley, G. Gloor, R. Siromoney, L. F. Landweber, L. F., In: C. Pandu Rangan, V. Raman, R. Ramanujam, (eds.), Foundations of Software Technology and Theoretical Computer Science, Springer Berlin Heidelberg, 269 (1999).
[4] H. Clausen-Schaumann, M. Rief, C. Tolksdorf, H. E. Gaub, Biophys. J. **78**(4), 1997 (2000).
[5] L. Polavarapu, J. Pérez-Juste, Q.-H. Xu, L. M. Liz-Marzán, J. Mater. Chem. C **2**(36), 7460 (2014).
[6] H.-P. Chiang, B. Mou, K. P. Li, P. Chiang, D. Wang, S. J. Lin, W. S. Tse, J. Raman Spectrosc. **32**, 45 (2001).
[7] Y. W. C. Cao, R. C. Jin, C. A. Mirkin, Science **297**, 1536 (2002).
[8] J. N. Anker, W. P. Hall, O. Lyandres, N. C. Shah, J. Zhou, R. P. van Duyne, Nat. Mater. **7**, 442 (2008).
[9] C. Fang, A. Agarwala, K. D. Buddharajua, Biosensors and Bioelectronics **24**, 216 (2008).
[10] W.-C. Lin, C. L. Chen, D. F. Hwang, R. Chang, J. S Hwang, H. P. Chiang, Plasmonics **4**, 178 (2009).
[11] K. C. Bantz, A. F. Meyer, H. S. Im, O. Kurtulus, S. H. Lee, N. C. Lindquist, S.-H. Oh, C. L. Haynes, Phys. Chem. Chem. Phys. **13**, 11551 (2011).
[12] W. Xie, S. Schlucker, Phys. Chem. Chem. Phys. **15**, 5329 (2013).
[13] W.-J. Chiu, T.-K. Ling, H.-P. Chiang, H.-J. Lin, C.-C. Huang, ACS Appl. Mater. Interfaces **7**, 8622 (2015).
[14] L. Guerrini, R. Arena, B. Mannini, F. Citi, R. Pini, P. Matteini, R. A. Alvarez-Puebla, ACS Appl. Mater. Interfaces **7**, 9420 (2015).
[15] S. Mirajkar, N. Maiti, P. Suprasanna, S. Kapoor, Journal of Raman Spectroscopy **51**(1), 89 (2019).
[16] Chunyang Zhou, Yanjun Yang, Haofei Li, Fei Gao, Chunyuan Song, Donglei Yang, Fan Xu, Na Liu, Yonggang Ke, Shao Su, and Pengfei Wang, Nano Lett. **20**(5), 3155 (2020).
[17] Weina Fang, Sisi Jia, Jie Chao, Liqian Wang, Xiaoyang Duan, Huajie Liu, Qian Li, Xiaolei Zuo, Lihua Wang, Lianhui Wang, Na Liu, Chuanhai Fan, Science advances **5**(9), 4506 (2019).
[18] P. T. Leung, W. S. Tse, Solid State Commun. **95**, 39 (1995).
[19] M. I. Stockman, Opt. Express **19**, 22029 (2011).
[20] B. Sharma, R. R. Frontiera, A. Henry, E. Ringe, R. P. van Duyne, Mater. Today **15**, 16 (2012).
[21] B. Draine, Astrophys. J. **333**, 848 (1988).
[22] U. Kreibig, Physik in unserer Zeit **39**(6), 281 (2008).
[23] C. Forestiere, G. Miano, S. V. Boriskina, L. D. Negro, Opt, Express **17**, 9648 (2009).

*Corresponding authors: e.taghavi@sutech.ac.ir; emami@sutech.ac.ir